PHYSICAL REVIEW B **67**, 121202(R) (2003)

Kinetically enhanced correlation and anticorrelation effects in self-organized quantum dot stacks

M. Meixner and E. Schöll
Institut für Theoretische Physik, Technische Universität Berlin, D-10623 Berlin, Germany
(Received 9 December 2002; published 6 March 2003)

We present kinetic Monte Carlo simulations explaining the correlation and anticorrelation effects observed in the self-organized growth of stacks of semiconductor quantum dots. Our simulations clarify the delicate interplay of kinetics and thermodynamics in strained heteroepitaxial semiconductor systems, and predict a sharp transition between correlated and anticorrelated growth as a function of the buffer thickness between the quantum dot layers. The vital role of the kinetically controlled and strain-mediated island size distributions is pointed out.

DOI: 10.1103/PhysRevB.67.121202 PACS number(s): 68.65.−k, 68.65.Hb, 81.16.Dn, 81.16.Rf

Self-assembled semiconductor quantum dots have emerged as a major challenge of nanoscience. They represent artificial atoms with unique controllable optoelectronic properties providing the basis for a novel generation of semiconductor devices.[1] For applications, it is desirable to have arrays of quantum dots with high density, narrow size distributions, and good spatial ordering. It has recently been demonstrated that regular three-dimensional superlattices of quantum dots with tunable lattice constants can be grown by using strain-mediated self-organization effects in the Stranski-Krastanov growth mode.[2] Stacks of islands organized in ordered patterns with both lateral and vertical correlations have been realized in different lattice-mismatched heteroepitaxial material systems.[3–11] There is evidence that stacks do not only increase the overall quantum dot density, but can also improve the size distribution and the spatial ordering. It is, however, difficult to control the growth since an intricate interplay of kinetic and thermodynamic effects comes into play, which may lead to crossover behavior as recently demonstrated by kinetic Monte Carlo simulations.[12] It has been shown that a thermodynamic equilibrium theory including the elastic strain can explain the alternating occurrence of vertical correlations and anticorrelations in multisheet arrays of two-dimensional islands as a function of spacer thickness,[13] but the effect of kinetics in these stacks is not well understood.

On the other hand, there is evidence[11] that ordered quantum dot stacks can be grown in the kinetically controlled regime without time consuming equilibration processes. Spatial ordering is obtained by depositing a large number of quantum dot layers on top of each other with thin buffer layers of substrate material in between. For those quantum dot stacks spatial ordering is increasing in parallel with the number of deposited layers. Here, the spatial correlation emerges in a system with no or only short periods of equilibration. Not only the spatial arrangement is enhanced, but also the uniformity of size, shape, and spacing of the dots can be improved.[2,14–18]

The strain field at the surface generated by the buried layers of quantum dots is responsible for the spatial ordering effect.[19] In the following, we present kinetic Monte Carlo (KMC) simulations incorporating self-consistently this strain field to model the growth of self-organized quantum dot stacks. Our simulation scheme goes well beyond other simulations,[14] where vertical alignment was observed leading to progressively increasing island sizes and spatial ordering. In contrast to the routine applied here, those results were obtained from strain calculations treating the buried islands as pointlike strain sources and from a nucleation model that places islands at strain energy minima but does not include diffusion processes.

We use the following approach. We start with a KMC simulation of the first layer of quantum dots, incorporating the elastic strain induced by the islands in a self-consistent way.[12] After the end of deposition, the ensemble is allowed to equilibrate for a certain time by strain-mediated diffusion before the islands are buried beneath a buffer layer of a certain thickness. The process of capping the islands with substrate material freezes the strain field and all diffusion processes are stopped. Hereafter the surface is again assumed to be flat but now the buried islands generate a nonhomogeneous strain field extending into the substrate surface. The actual strength of the strain is calculated self-consistently from elasticity theory with the buried islands as the sources of strain. Then another deposition process is started and a new layer of quantum dots is modeled by KMC, now subjected to two sources of strain, i.e., the buried islands and the islands in the surface layer.

Of course, the strain at the surface of a stack of quantum dots is not only determined by the topmost buried layer but all the buried layers beneath contribute to the surface strain, albeit with decreasing relevance. In the following simulations, the strain induced by the respective top five layers is taken into account.

Our event-based KMC simulations[20–23] use a solid-on-solid model with deposition and diffusion as the relevant processes. Diffusion of adatoms occurs on a square lattice by nearest-neighbor hopping. Atoms can cross island edges by surmounting a Schwöbel barrier $E_{SW}=0.1$ eV. The relevant energies in our simulations are the binding energy to the surface $E_s=1.3$ eV and the strength of the $n\leqslant 4$ nearest-neighbor bonds $E_b=0.3$ eV that influence the time scale for diffusion and island formation, respectively. We use values of the energy parameters that are typical for a variety of semiconducting materials and have been used in other KMC simulations.[24] Systematic investigations of the effects of variation of these energies have been reported.[25–28] In order to keep the number of free parameters at a minimum, we use a simple single-species KMC model with effective energies E_s, E_b. It should be noted that these energies scale with the

growth temperature, since only the quotient of energy barrier and temperature appears in the transition rates. It is an advantage of our general results that they can be applied to a variety of material systems by simultaneously rescaling the diffusion barriers and growth temperatures.

Existing islands generate an elastic strain field caused by the lattice mismatch. This strain field facilitates detachment from island boundaries and the motion of adatoms in the vicinity of islands through a position-dependent energy correction term $E_{str}(x,y)$, which decreases the binding energy.

The hopping rate for a single atom is then given by an Arrhenius law $p=\nu\exp[-(E_s+nE_b-E_{str})/kT]$ with the attempt frequency[29–31] $\nu=10^{13}$ s^{-1}, temperature T, and Boltzmann's constant k. The three-dimensional strain field

$$\epsilon_{ij}(\boldsymbol{r})=\frac{1}{2}\left(\frac{\partial u_i}{\partial x_j}+\frac{\partial u_j}{\partial x_i}\right) \tag{1}$$

is treated in the framework of the continuum theory of elastic media using the static Green's tensor $G_{ij}(\boldsymbol{r},\boldsymbol{r}')$ to calculate the elastic displacements $u_i(\boldsymbol{r})$:

$$u_i(\boldsymbol{r})=-\oint_S d^2r' G_{ij}(\boldsymbol{r},\boldsymbol{r}')P_j(\boldsymbol{r}') \tag{2}$$

The line forces $P_i(\boldsymbol{r})$ appear at the island edges and act as the sources of the strain. Therefore, the integration is carried out along all island boundaries S. The strain energy is then calculated from the displacements in isotropic approximation:[32]

$$E_{str}=\frac{\lambda}{2}\left(\sum_i \epsilon_{ii}\right)^2+\mu\sum_{ij}\epsilon_{ij}^2 \tag{3}$$

with elastic constants $\lambda=0.32\times10^{12}$ erg/cm^3 and $\mu=0.54\times10^{12}$ erg/cm^3 corresponding to GaAs. The strain field is vital in inducing cooperative growth with a well-defined average island size rather than Ostwald ripening,[22] but the results do not depend sensitively upon the precise values of the parameters λ and μ, since the strain field decays fast with increasing distance from the island boundaries.

Note that in our KMC simulations the wetting layer is not explicitly taken into account. Therefore, the effective buffer layer thickness used in the simulations includes the wetting layer. Transfer of material from the wetting layer to the dots which might occur for very thin buffer layers is disregarded. Also, only the fundaments of the quantum dots (monolayer islands) in each stack layer are modeled by KMC, and structural changes in the shape and size of quantum dots during the overgrowth process are not considered. It is, however, assumed that the main contribution to the surface strain field does not originate from morphological details but is given by the position and lateral size of the dots. Indeed, vertical correlation effects in stacks of two-dimensional submonolayer islands have also been observed experimentally.[33]

As a measure for vertical correlation or anticorrelation in stacked quantum dot layers we calculate the pairing probability P_p, which indicates the ratio of islands that have grown directly above another island. To this end the centers of mass of the surface islands and of the islands of the topmost buried layer are determined. Then, for each surface island the lateral distance to the position vertically above the nearest island in the buried layer d'_{nn} is calculated. Its average $\overline{d'_{nn}}$ is normalized by the maximum average distance possible for islands on a square lattice: $\overline{d_{nn}}/\sqrt{2}$, where $\overline{d_{nn}}$ is the average distance between islands in the surface layer. Thus the pairing probability is defined as

$$P_p:=1-\sqrt{2\overline{d'_{nn}}/\overline{d_{nn}}}. \tag{4}$$

Perfect correlation or anticorrelation correponds to $P_p=1$ or $P_p=0$, respectively, while uncorrelated growth is associated with $P_p=0.5$.

The key ingredient for vertical correlation of quantum dot layers is the strain field at the surface of the stack produced by the buried islands. The nonhomogeneous strain increases the probability of island nucleation at certain positions. To allow for nucleation to take place at these distinguished places, the flux to the surface during deposition should not be chosen too high so that nucleation is driven rather by aggregation of adatoms at energetically favored places than by accidental nucleation processes due to a high overall monomer density. After deposition the island configuration is given 20 s of time to equilibrate before overgrowing the island layer and thus freezing the three-dimensional strain field.

To show the increase in spatial ordering with the increase of deposited layers, a stack of islands consisting of 150 single layers was simulated. After each deposited layer of islands having a coverage of 35% each, the pairing probability P_p was calculated. The spacer thickness was chosen to be 15 ML. The resulting dependence of P_p on the number of deposited layers is shown in Fig. 1(a). For the first few layers the pairing probability is close to 0.5 indicating uncorrelated growth. From the fifth layer on the pairing probability clearly tends towards larger values, which is a sign of correlated island growth. After the deposition of 20 layers, the pairing probability reaches a saturation value of 0.8. For all further simulations a stack of 20 layers has been assumed.

For the above simulation with a buffer layer thickness of 15 ML as well as for two equivalent simulations with 5 and 30 ML spacer thickness, respectively, we find that with increasing number of deposited layers the island size distribution shifts towards larger island sizes. This effect is most pronounced for thin buffer layers. The shift in the average island size can be understood as the approach towards thermodynamic equilibrium.[12] The additional strain from the buried layers enhances the mobility of the diffusing adatoms with increasing stack height, which is equivalent to an increase in temperature. A higher growth temperature, on the other hand, means a faster evolution towards equilibrium. Additionally, the inhomogeneous strain field creates preferred nucleation sites for islanding at places of reduced strain. This effect induces a spatial correlation between the growing layer and the buried layers again promoting equilibration of the islands. The average island size is, however, in all cases still distinctly below the equilibrium size [formula (3) in Ref. 12]. The effect of strain is reduced for thick buffer

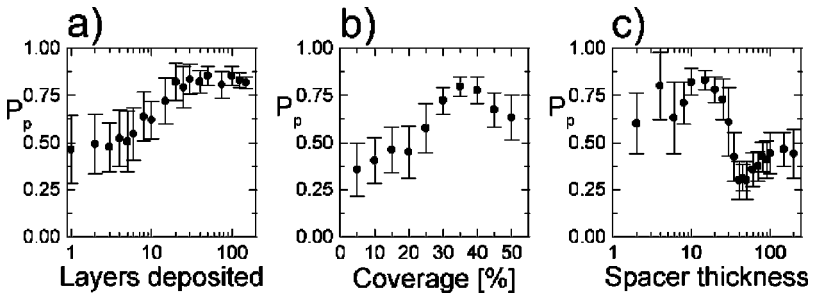

FIG. 1. Pairing probability P_p in dependence of (a) the number of deposited quantum dot layers for a spacer thickness of 15 ML, (b) the surface coverage c (excluding the wetting layer) for a spacer thickness of ten ML, (c) the spacer thickness (number of ML). The error bars denote the variance of the pairing probability ($T=700$ K, $F=0.02$ ML/s, $c=35\%$, stack of 20 quantum dot layers in (b) and (c), simulation time 37.5 s/layer, 250×250 grid).

layers, hence the acceleration of the equilibration process is less pronounced for thicker spacers.

The dependence of the pairing probability on the total coverage of the island ML has been studied by computing the pairing probability after the growth of 20 stacked island layers with varying coverage and a constant buffer layer thickness of ten ML. The result is shown in Fig. 1(b).

For very low coverages below 10% the pairing probability indicates anticorrelated growth. As a result of the low coverage, the distance between islands is comparatively large and, hence, the areas of strain induced by the buried islands do not overlap. Thus, adatoms are driven away from areas atop buried islands and nucleation takes place favorably in between buried islands, where the strain field is lowest. This consequently leads to anticorrelated growth. For a coverage above 10% the growth proceeds uncorrelated. For coverages above 25% the growth mode changes to correlated growth. Here, the strain between the islands is strong due to decreasing island separation with increasing coverage. Now the nucleation directly above buried islands becomes more favorable, since here the surface is only weakly strained. This can be understood by looking at the strain generated at the island boundaries. The strain discontinuity along the boundary of large islands induces a constant strain at the island center which is usually weaker than the strain in between islands if the coverage is high enough. The pairing probability in Fig. 1(b) has a maximum at a coverage of $c=35\%$. Further increase of the coverage leads to clustering of islands and the correlation effect is reduced again. For the following simulations, the optimum coverage of 35% has been chosen in order to obtain a maximum correlation effect.

Next, we investigate the dependence of the pairing probability on spacer thickness [Fig. 1(c)]. For a spacer thickness of less than 15 ML the growth is correlated. With increasing buffer layer thickness a sharp transition between correlated and anticorrelated growth occurs between 25 and 35 ML, yielding pronounced anticorrelation at around 40 ML. Subsequently with increasing buffer thickness correlation effects decay, and uncorrelated growth with $P_p\approx0.5$ is observed for spacers thicker than some 60–70 ML. Then the strain fields of the buried islands are too weak to influence the surface kinetics of diffusing adatoms significantly.

In the correlated growth regime, the least strained regions, where the diffusivity is lowest, and, hence, nucleation of islands is favored, are areas above centers of buried islands. As a consequence, correlated growth can be observed for thin buffer layers and large islands. In Fig. 2(a), the evolution of the pairing probability in dependence of the number of grown island layers is shown. The buffer layer thickness for this simulation was chosen as 5 ML. For the first few layers the growth is uncorrelated and then becomes increasingly correlated up to the 18th layer, where the pairing probability reaches saturation and remains almost constant at a value of $P_p\approx0.8$. In the insets the island distributions of the topmost three island layers are shown to demonstrate the spatial correlation in the vertical direction.

The interplay of spacer thickness and island size might also explain why correlated growth is not instantly observed. For the first few island layers the growth is uncorrelated but the size distribution shifts considerably towards larger islands finally giving rise to correlated growth as seen in Fig. 2(a).

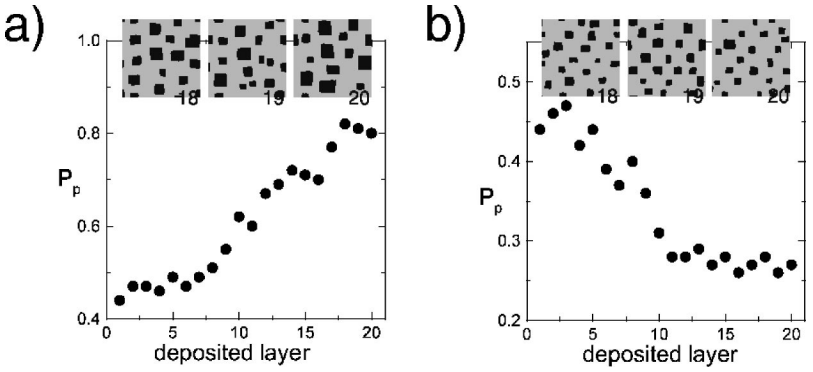

FIG. 2. a) Evolution of pairing probability versus the number of deposited quantum dot layers for the case of correlated growth (spacer thickness 5 ML). The inset shows the three topmost quantum dot layers. ($T=700$ K, $F=0.01$ ML/s, $c=35\%$, stack of 20 layers, simulation time 37.5 s/layer). (b) Same as in (a) for the case of anticorrelated growth (spacer thickness 40 ML).

For large buffer layer thickness the buried islands appear as point sources of strain and the strain field at the surface has a maximum value vertically above the island center. Nucleation of islands at the surface is consequently enhanced *between* the islands and anticorrelated growth is observed. Since this growth mode does not depend on the lateral extension of the buried islands as sensitively as the correlated growth does, the onset of anticorrelated growth is already visible for the first few grown island layers in Fig. 2(b). After ten deposited island layers the pairing probability reaches saturation at a value of ≈ 0.26. The insets show the top three island layers of the stack, clearly exhibiting anticorrelation.

In conclusion, we have shown by kinetic Monte Carlo simulations that successive overgrowth of island layers with substrate material under the assumption of an extended strain field leads to an improvement of the self-organized size ordering and spatial arrangement of the islands. Vertical correlation and anticorrelation effects can be induced in the kinetically controlled growth regime by deposition and diffusion processes without equilibrating the system for long periods of time.

In order to obtain best results for correlated growth with narrow size distributions for a given material, one should first determine the optimum coverage according to Fig. 1(b). Then the buffer layer thickness should be chosen sufficiently thin according to Fig. 1(c). Apart from the spacer thickness, correlation depends on the average size of the buried islands which also increases during the stacking process. Thus, the self-organized increase in average island size assists the growth of correlated stacks of islands. For intermediate spacer thickness anticorrelated growth can be observed, while for very thick spacer layers no correlation at all occurs. This is in good agreement with experiments.[10,34] Our kinetic simulations may also explain the observation[11] that vertical correlations can result from variations in strain energy by the order of 1 meV, which is a much smaller energy difference than would be required for thermodynamic equilibrium considerations; this stresses the vital role of kinetics. Moreover, in systems with low growth temperatures equilibrium might practically never be reached since reasonable equilibration times would have to be of the order of weeks or even months.

We are grateful to F. Elsholz, R. Kunert, and V. A. Shchukin for discussion. Support by the Deutsche Forschungsgemeinschaft in the framework of Sfb 296 is acknowledged.

[1] D. Bimberg, M. Grundmann, and N. Ledentsov, *Quantum Dot Heterostructures* (Wiley, New York, 1999).
[2] G. Springholz, V. Holý, M. Pinczolits, and G. Bauer, Science **282**, 734 (1998).
[3] L. Goldstein, F. Glas, J.Y. Marzin, M.N. Charasse, and G.L. Roux, Appl. Phys. Lett. **47**, 1099 (1985).
[4] T.S. Kuan and S.S. Iyer, Appl. Phys. Lett. **59**, 2242 (1991).
[5] J.Y. Yao, T.G. Andersson, and G.L. Dunlop, J. Appl. Phys. **69**, 2224 (1991).
[6] Q. Xie, A. Madhukar, P. Chen, and N.P. Kobayashi, Phys. Rev. Lett. **75**, 2542 (1995).
[7] G.S. Solomon, J.A. Trezza, A.F. Marshall, and J.S. Harris, Phys. Rev. Lett. **76**, 952 (1996).
[8] N.N. Ledentsov, V.A. Shchukin, M. Grundmann, N. Kirstaedter, J. Böhrer, O. Schmidt, D. Bimberg, V.M. Ustinov, A.Y. Egorov, A.E. Zhukov, P.S. Kop'ev, S.V. Zaitsev, N.Y. Gordeev, Z.I. Alferov, A.I. Borovkov, A.O. Kosogov, S.S. Ruvimov, P. Werner, U. Gösele, and J. Heydenreich, Phys. Rev. B **54**, 8743 (1996).
[9] F. Heinrichsdorff, M.-H. Mao, N. Kirstaedter, A. Krost, D. Bimberg, A.O. Kosogov, and P. Werner, Appl. Phys. Lett. **71**, 22 (1997).
[10] V. Holý, G. Springholz, M. Pinczolits, and G. Bauer, Phys. Rev. Lett. **83**, 356 (1999).
[11] G. Springholz, M. Pinczolits, P. Mayer, V. Holy, G. Bauer, H. Kang, and L. Salamanca-Riba, Phys. Rev. Lett. **84**, 4669 (2000).
[12] M. Meixner, E. Schöll, V.A. Shchukin, and D. Bimberg, Phys. Rev. Lett. **87**, 236101 (2001); **88**, 059901 (2002).
[13] V.A. Shchukin, D. Bimberg, V.G. Malyshkin, and N.N. Ledentsov, Phys. Rev. B **57**, 12 262 (1998).
[14] J. Tersoff, C. Teichert, and M.G. Lagally, Phys. Rev. Lett. **76**, 1675 (1996).
[15] A.-L. Barabási, Appl. Phys. Lett. **70**, 764 (1997).
[16] H. Eisele, O. Flebbe, T. Kalka, C. Preinesberger, F. Heinrichsdorff, and A. Krost, Appl. Phys. Lett. **75**, 106 (1999).
[17] F. Liu, S.E. Davenport, H.M. Evans, and M.G. Lagally, Phys. Rev. Lett. **82**, 2528 (1999).
[18] M. Pinczolits, G. Springholz, and G. Bauer, Phys. Rev. B **60**, 11 524 (1999).
[19] Q. Xie, P. Chen, and A. Madhukar, Appl. Phys. Lett. **65**, 2051 (1994).
[20] A.B. Bortz, M.H. Kalos, and J.L. Lebowitz, J. Comp. Physiol. **17**, 10 (1975).
[21] A. Madhukar, Surf. Sci. **132**, 344 (1983).
[22] E. Schöll and S. Bose, Solid-State Electron. **42**, 1587 (1998).
[23] K.E. Khor and S.D. Sarma, Phys. Rev. B **62**, 16 657 (2000).
[24] S. Clarke, M.R. Wilby, and D.D. Vvedensky, Surf. Sci. **255**, 91 (1991).
[25] T. Shitara, D. Vvedensky, M. Wilby, J. Zhang, J.H. Neave, and B. Joyce, Phys. Rev. B **46**, 6815 (1992).
[26] P. Smilauer and D. Vvedensky, Phys. Rev. B **48**, 17 603 (1993).
[27] C. Heyn and M. Harsdorff, Phys. Rev. B **55**, 7034 (1997).
[28] K. Morgenstern, E. Lægsgaard, and F. Besenbacher, Phys. Rev. B **66**, 115408 (2002).
[29] L. Nurminen, A. Kuronen, and K. Kaski, Phys. Rev. B **63**, 035407 (2000).
[30] M. Larsson, Phys. Rev. B **64**, 115428 (2001).
[31] J. Krug, Physica A (to be published 2002).
[32] L.D. Landau and E.M. Lifshitz, *Theory of Elasticity* (Pergamon, New York, 1970).
[33] N.N. Ledentsov, I.L. Krestnikov, M.V. Maximov, S.V. Ivanov, S.L. Sorokin, P.S. Kop'ev, Z.I. Alferov, D. Bimberg, and C.M.S. Torres, Appl. Phys. Lett. **70**, 2766 (1997).
[34] M. Strassburg, V. Kutzer, U.W. Pohl, A. Hoffmann, I. Broser, N.N. Ledentsov, D. Bimberg, A. Rosenauer, U. Fischer, D. Gerthsen, I.L. Krestnikov, M.V. Maximov, P.S. Kop'ev, and Z.I. Alferov, Appl. Phys. Lett. **72**, 942 (1998).